06.1; 09.1

Optical properties of volcano-shaped gold-silicon structures fabricated by femtosecond laser exposure

© E.Yu. Ponkratova[1], E.I. Ageev[1], M.V. Zhukov[2], A.O. Larin[1], I.S. Mukhin[3,4], D.A. Zuev[1]

[1] ITMO University, St. Petersburg, Russia
[2] Institute of Analytical Instrument Making, Russian Academy of Sciences, St. Petersburg, Russia
[3] Alferov Federal State Budgetary Institution of Higher Education and Science Saint Petersburg National Research Academic University of the Russian Academy of Sciences, St. Petersburg, Russia
[4] Peter the Great Saint-Petersburg Polytechnic University, St. Petersburg, Russia
E-mail: eiageev@itmo.ru

Received March 27, 2023
Revised May 2, 2023
Accepted May 2, 2023

Here, we experimentally study the photoluminescence of volcano-shaped hybrid structures created from a bi-layer gold−silicon film exposed by several femtosecond laser pulses at a wavelength of 1048 nm. The external and phase composition of the obtained structures were analyzed by a combination of atomic force microscopy and Raman studies. The damage threshold is found and the stability of the broadband photoluminescence of such structures is demonstrated.

Keywords: Gold−silicon nanostructures, femtosecond laser irradiation, broadband photoluminescence.

DOI: 10.61011/TPL.2023.07.56435.19568

Ever since their first demonstration by Nakata et al. [1] and Chichkov et al. [2], femtosecond laser pulses have provided an excellent opportunity for fabricating a wide range of subwavelength microstructures in thin metallic films on glass substrates.

In the general case, thermal stresses are induced in a film when the surface of a thin metallic layer is irradiated by a low-intensity strongly focused femtosecond laser pulse. This results in the formation of nanovoids of a parabolic shape (nanobumps) or (at higher pulse energies) nanocones and nanoapertures [3,4]. The majority of published studies have been focused on the geometric and dimensional features of structures made of noble metals and demonstrated the possibility of tuning their resonance by the pulse energy [5] or the film thickness [6]. Ordered arrays of such structures may serve as optical sensors [7], security labels [8], or nonlinear media for second-harmonic generation (SHG) [9]. However, plasmonic materials have intrinsically high losses due to heating at optical frequencies. A the same time, dissipative losses in dielectric materials with a high refraction index, such as silicon and germanium, are negligible. A combination of plasmonic and dielectric components in a single hybrid nanostructure should allow one to get the best of both worlds [10].

The easiest way to fabricate hybrid structures consists in subjecting a two-layer gold−silicon film to laser pulses. Specifically, various metal–dielectric structures demonstrate both efficient SHG and broadband photoluminescence (PL) in the visible range (e.g., hybrid nanosponges [11] and other laser-induced structures [12]). As was demonstrated in [13], nanobumps form on a two-layer silicon−gold film subjected to irradiation. As the power density increases, these nanobumps transform into volcano-shaped structures. In the present study, the internal composition of volcano-shaped structures is examined using Raman spectroscopy and energy-dispersive X-ray spectroscopy (EDXS) in the scanning transmission electron microscopy (STEM) mode, and their external geometry is studied by atomic force microscopy (AFM) and scanning electron microscopy (SEM). In addition, the stability of their broadband PL is demonstrated.

Structures were fabricated using a TEMA-150 ($\lambda = 1048$ nm, $\tau = 150$ fs) femtosecond laser source with a repetition rate (RR) of 1 Hz after a pulse selector based on a Pockels cell. Laser pulses were focused at the top surface of a film by a Mitutoyo M Plan Apo NIR ($10\times$, NA $= 0.26$) objective into a spot with $1/e$ diameter $d \sim 4.9\,\mu$m from the substrate side. Two-layer Au (30 nm)/Si (90 nm) films on a glass substrate were used. Structure formation proceeded after irradiation with five laser pulses at an absorbed power density on the order of 19 ± 3 mJ/cm^2.

SEM and AFM studies were carried out to characterize the morphology and external geometry of structures (Fig. 1, *a*). The AFM image was obtained using an Ntegra Aura microscope in the semi-contact mode with passive and active vibration protection systems and HA_NC probes. Raman spectroscopy was performed to examine the phase transformations of the silicon structure component. Spectra were recorded under excitation by a He−Ne laser with a wavelength of 632.8 nm, which was focused at the surface by a Mitutoyo M Plan Apo NIR ($100\times$, NA $= 0.7$) objective. The Raman signal was collected by the same objective and projected onto a DU 420A-OE 325

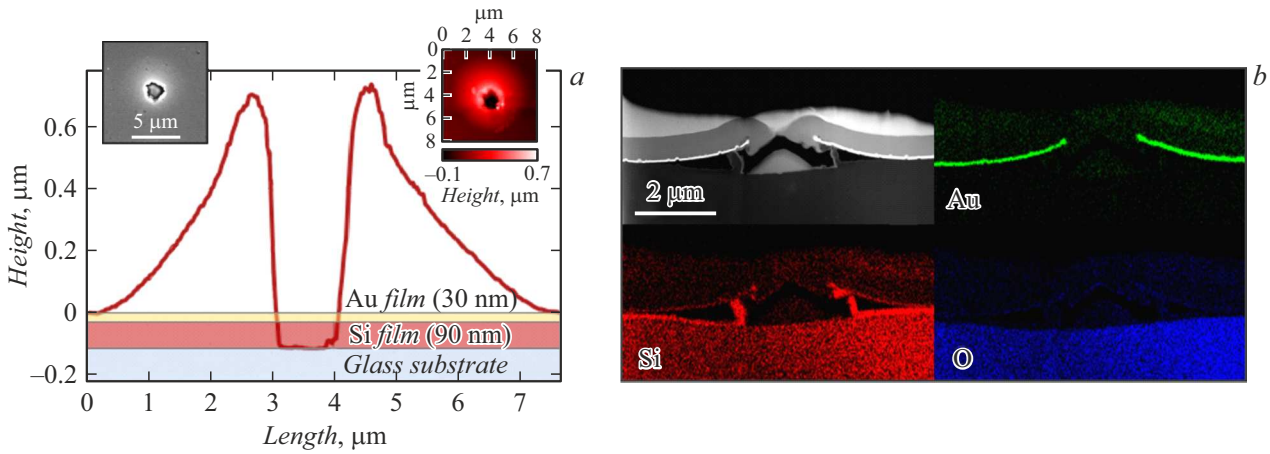

Figure 1. *a* — Profile of the hybrid nanostructure determined based on AFM data. SEM and AFM images are shown in the insets; *b* — STEM image of the cross section of the hybrid nanostructure and EDXS maps of the elemental composition.

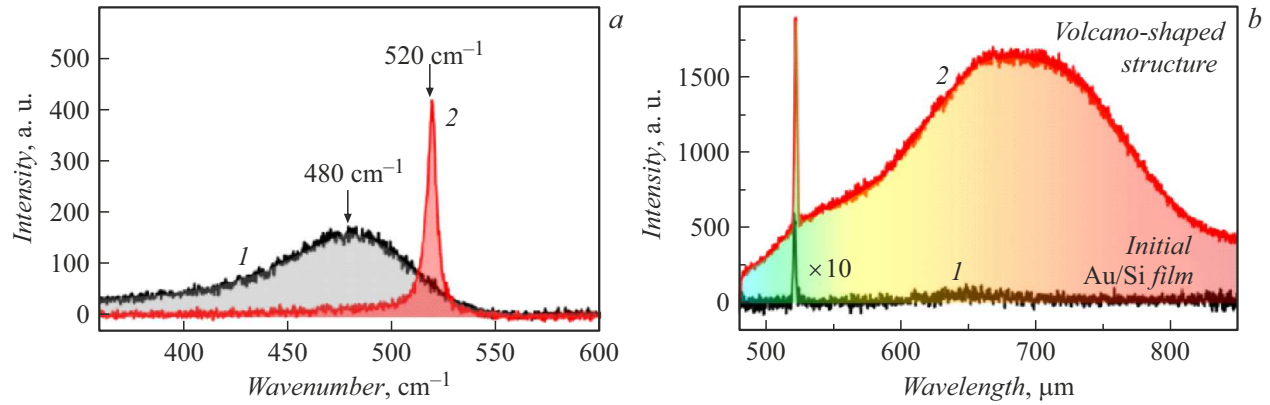

Figure 2. Characteristic Raman (*a*) and PL/SHG (*b*) spectra of the initial Au/Si film (*1*) and volcano-shaped structures (*2*).

CCD array through a LabRam HR spectrometer with a 600 lines/mm diffraction grating.

In order to visualize the redistribution of gold and silicon, lamellae were cut form the obtained structures by the focused ion beam of a FEI Helio Nanolab 600i microscope, and EDXS mapping of the elemental composition in the STEM mode was performed using a JEOL ARM200 microscope with a JEOL Centurio detector (Fig. 1, *b*). A Pt layer was deposited in advance onto the sample surface to protect it in the process of cutting. In contrast to [4], the obtained volcano-shaped structures do not feature a radial redistribution of thickness of the gold film (presumably, due to detachment of the thickened section at the structure center).

The nonlinear optical properties of the obtained structures were characterized by recording PL and SHG signals under pumping by radiation from a TEMA-150 (RR = 80 MHz) laser source. The laser radiation power was varied within the 1–30 mW range using an attenuator. Radiation was focused by a Mitutoyo M Plan Apo NIR (100×, NA = 0.7) objective. PL and SHG signals were collected by the same objective, while reflected pumping radiation was blocked by a FELH 850 filter; a 150 lines/mm diffraction grating was used to record the spectra.

It follows from Fig. 2, *a* that the initial Au/Si film has a broadband signal with a peak around 480 cm^{-1}, which corresponds to the amorphous phase. The presence of an intense Raman peak around 520 cm^{-1} confirms that silicon starts crystallizing in the course of formation of hybrid structures. In turn, modification of the crystal structure induces a change in the optical properties (Fig. 2, *b*) due to the injection of hot electrons and holes that are generated in gold as a result of multiphoton absorption in the silicon component with subsequent recombination [14]. The initial film emits only a weak SHG signal at a wavelength of 524 nm. SHG is forbidden in centrosymmetric materials such as gold, although this symmetry may be violated at the surface and amplified by certain surface defects [15]. The volcano-shaped structure (Fig. 2, *b*) produces much stronger SHG and PL signals. This may be attributed to the transparency of the central section of the structure, where its emission is not absorbed by gold.

Figure 3, *a* presents the evolution of PL spectra of the hybrid structure under different pumping power levels.

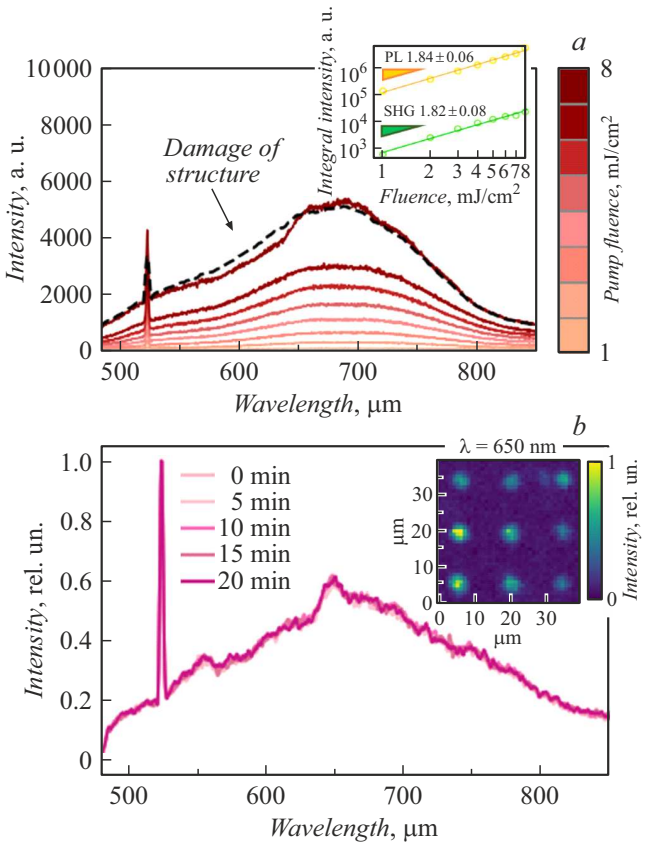

Figure 3. *a* — PL spectra of volcano-shaped structures under different pumping levels. The dependence of the SHG and PL signal intensity on the pumping energy density is shown in the inset. *b* — Stability of PL spectra under a pumping energy density of 4.9 mJ/cm^2. The broadband PL map for a 3×3 array of structures is shown in the inset (the sample being mapped was shifted by piezo positioning stages with a pitch of 500 nm to collect the PL signal at each point). A color version of the figure is provided in the online version of the paper.

The spectrum shape remains stable up to the damage threshold at an energy density of ~ 7.9 mJ/cm^2. Below this level, the spectrum intensity increases continuously with pumping power; when the structure gets damaged, the characteristic shape of its spectrum changes (dashed curve in Fig. 3, *a*). The slope of the dependence of the SHG and PL signal intensity on the pumping energy density (inset in Fig. 3, *a*) suggests that both processes are induced by two-photon absorption. Since the stability of optical response is crucial for practical applications, PL spectra were measured repeatedly with a pitch of 5 min within an interval of 20 min (Fig. 3, *b*). In addition, an array of structures was recorded (inset in Fig. 3, *b*) to examine the consistency of fabrication of structures and characterize the nonlinear signal distribution along them. It can be seen that the intensity of broadband PL signals increases toward the center of structures and varies somewhat from one structure to the other.

Thus, hybrid volcano-shaped structures with a strong nonlinear optical response were fabricated on a two-layer gold–silicon film. A complex of SEM, STEM, Raman, and AFM studies with EDXS mapping of the elemental composition revealed the onset of crystallization of initially amorphous silicon and detachment of the two-layer film from the substrate, resulting in the formation of an aperture at the center of the irradiated region. Hybrid structures feature intense broadband PL within the spectral range of 480–850 nm under laser pumping up to the damage threshold at 7.9 mJ/cm^2; the PL signal remains stable below this level. It should be noted in conclusion that arrays of such structures hold promise for application as efficient nonlinear sources to be used in visualization of biological objects and nanospectroscopy.

Acknowledgments

The authors wish to thank S. Bruyère (Institut Jean Lamour, CNRS — Université de Lorraine) for STEM/EDXS measurements.

Funding

This study was supported by the Russian Science Foundation (grant No. 19-79-10259, https://rscf.ru/en/project/19-79-10259/).

Conflict of interest

The authors declare that they have no conflict of interest.

References

[1] Y. Nakata, T. Okada, M. Maeda, Jpn. J. Appl. Phys., **42**, L1452 (2003). DOI: 10.1143/JJAP.42.L1452
[2] F. Korte, J. Koch, B.N. Chichkov, Appl. Phys. A, **79**, 879 (2004). DOI: 10.1007/s00339-004-2590-5
[3] V.V. Zhakhovskii, N.A. Inogamov, Yu.V. Petrov, S.I. Ashitkov, K. Nishihara, Appl. Surf. Sci., **255**, 9592 (2009). DOI: 10.1016/j.apsusc.2009.04.082
[4] X.W. Wang, A.A. Kuchmizhak, X. Li, S. Juodkazis, O.B. Vitrik, Yu.N. Kulchin, V.V. Zhakhovsky, P.A. Danilov, A.A. Ionin, S.I. Kudryashov, A.A. Rudenko, N.A. Inogamov, Phys. Rev. Appl., **8**, 044016 (2017). DOI: 10.1103/PhysRevApplied.8.044016
[5] D.V. Pavlov, A.Yu. Zhizhchenko, M. Honda, M. Yamanaka, O.B. Vitrik, S.A. Kulinich, S. Juodkazis, S.I. Kudryashov, A.A. Kuchmizhak, Nanomaterials, **9**, 1348 (2019). DOI: 10.3390/nano9101348
[6] M. Reininghaus, D. Wortmann, Z. Cao, J.M. Hoffmann, T. Taubner, Opt. Express, **21**, 32176 (2013). DOI: 10.1364/OE.21.032176
[7] A. Kuchmizhak, O. Vitrik, Yu. Kulchin, D. Storozhenko, A. Mayor, A. Mirochnik, S. Makarov, V. Milichko, S. Kudryashov, V. Zhakhovsky, N. Inogamov, Nanoscale, **8**, 12352 (2016). DOI: 10.1039/C6NR01317A

[8] V. Lapidas, A. Zhizhchenko, E. Pustovalov, D. Storozhenko, A. Kuchmizhak, Appl. Phys. Lett., **120**, 261104 (2022). DOI: 10.1063/5.0091213
[9] A.B. Cherepakhin, D.V. Pavlov, I.I. Shishkin, P.M. Voroshilov, S. Juodkazis, S.V. Makarov, A.A. Kuchmizhak, Appl. Phys. Lett., **117**, 041108 (2020). DOI: 10.1063/5.0016173
[10] S. Kruk, M. Weismann, A.Yu. Bykov, E.A. Mamonov, I.A. Kolmychek, T. Murzina, N.C. Panoiu, D.N. Neshev, Yu.S. Kivshar, ACS Photon., **2**, 1007 (2015). DOI: 10.1021/acsphotonics.5b00215
[11] A.O. Larin, A. Nominé, E.I. Ageev, J. Ghanbaja, L.N. Kolotova, S.V. Starikov, S. Bruyère, T. Belmonte, S.V. Makarov, D.A. Zuev, Nanoscale, **12**, 1013 (2020). DOI: 10.1039/C9NR08952G
[12] S.O. Gurbatov, V. Puzikov, D. Storozhenko, E. Modin, E. Mitsai, A. Cherepakhin, A. Shevlyagin, A.V. Gerasimenko, S.A. Kulinich, A.A. Kuchmizhak, ACS Appl. Mater. Interfaces, **15**, 3336 (2023). DOI: 10.1021/acsami.2c18999
[13] E. Ponkratova, E. Ageev, P. Trifonov, P. Kustov, M. Sandomirskii, M. Zhukov, A. Larin, I. Mukhin, T. Belmonte, A. Nominé, S. Bruyère, D. Zuev, Adv. Funct. Mater., **32**, 2205859 (2022). DOI: 10.1002/adfm.202205859
[14] B.I. Afinogenov, A.N. Sofronov, I.M. Antropov, N.R. Filatov, A.S. Medvedev, A.S. Shorokhov, V.N. Mantsevich, N.S. Maslova, T. Kim, E. Jeang, I. Kim, M. Seo, K. Han, S. Bae, W. Joo, H. Yoo, V.O. Bessonov, A.A. Fedyanin, M.V. Ryabko, S.V. Polonsky, Opt. Lett., **46**, 3071 (2021). DOI: 10.1364/OL.424834
[15] A.V. Zayats, T. Kalkbrenner, V. Sandoghdar, J. Mlynek, Phys. Rev. B, **61**, 4545 (2000). DOI: 10.1103/PhysRevB.61.4545

Translated by D.Safin